Supporting Information for

Nickel(II) Complexes with Covalently Attached Quinols Rely on Ligand-Derived Redox Couples to Catalyze Superoxide Dismutation

Robert Boothe,[†,a] Julian Oppelt,[‡,§,a] Alicja Franke,[‡,§] Jamonica L. Moore,[†] Andrea Squarcina,[‡] Achim Zahl,[§] Laura Senft,[‡] Ina Kellner,[‡] Akudo L. Awalah,[†] Alisabeth Bradford,[†] Segun V. Obisesan,[†] Dean D. Schwartz,[¥] Ivana Ivanović-Burmazović,[‡,*] and Christian R. Goldsmith[†,*]

[†]Department of Chemistry and Biochemistry, Auburn University, Auburn, AL 36849, USA
[‡]Department of Chemistry, Ludwig-Maximilians-Universität München, 81377 München, Germany
[§]Department of Chemistry and Pharmacy, Friedrich-Alexander-Universität Erlangen-Nürnberg, Egerlandster. 1, 91508 Erlangen, Germany
[¥]Department of Anatomy, Physiology, and Pharmacology, College of Veterinary Medicine, Auburn University, Auburn, AL 36849, USA

*Corresponding authors: Ivana.Ivanovic-Burmazovic@cup.uni-muenchen.de, crgoldsmith@auburn.edu

[a]These authors contributed equally to the manuscript.

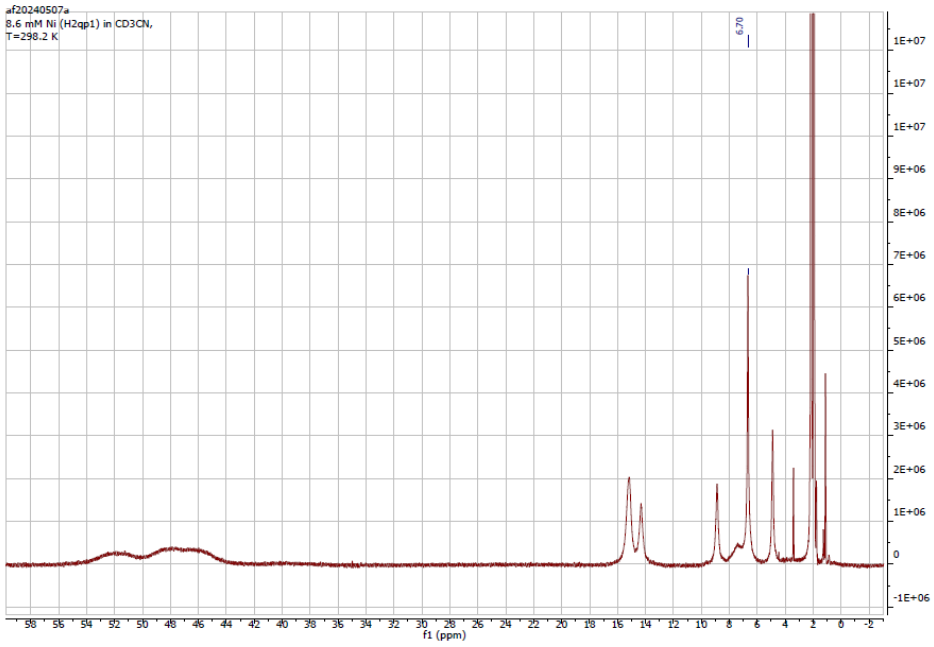

A

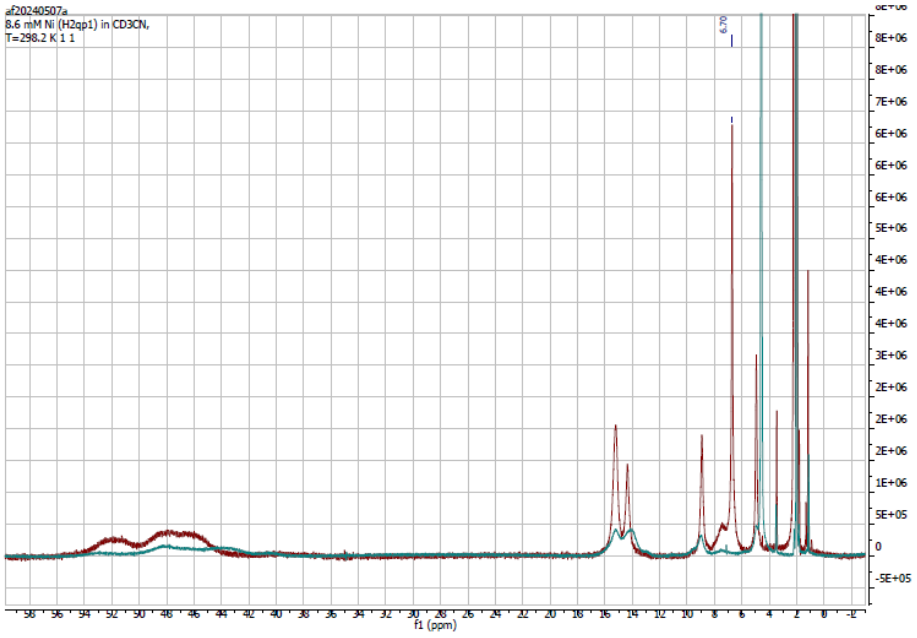

B

Figure S1. A) ^{1}H NMR data (400 mHz, 294 K) for a 6.8 mM sample of **1** in CD_3CN. B) Comparison of data from panel A (brown) to spectrum obtained for 6.8 mM sample of **1** in 20% CD_3CN/80% D_2O (blue). The presence of D_2O causes the feature at 6.7 ppm to vanish.

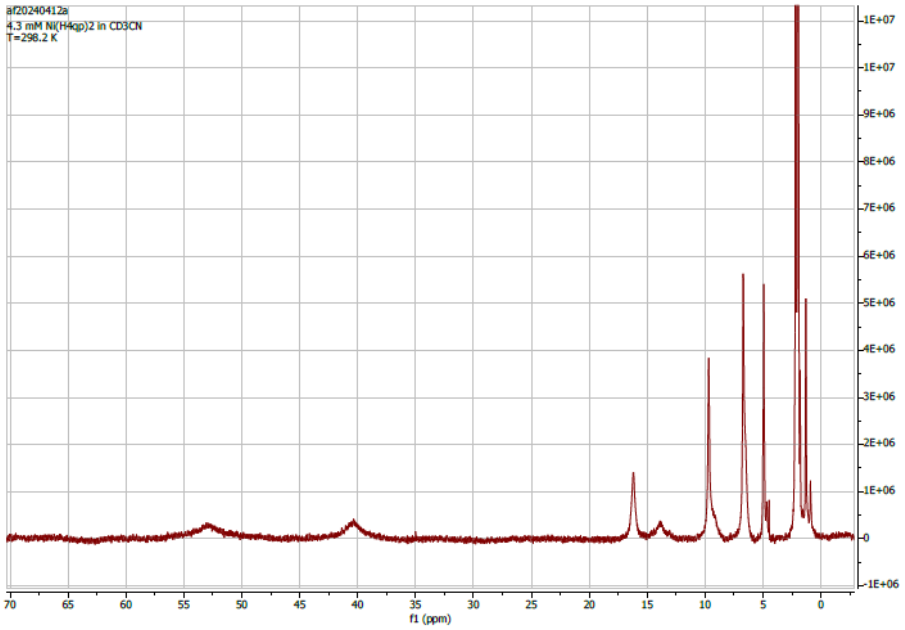

A

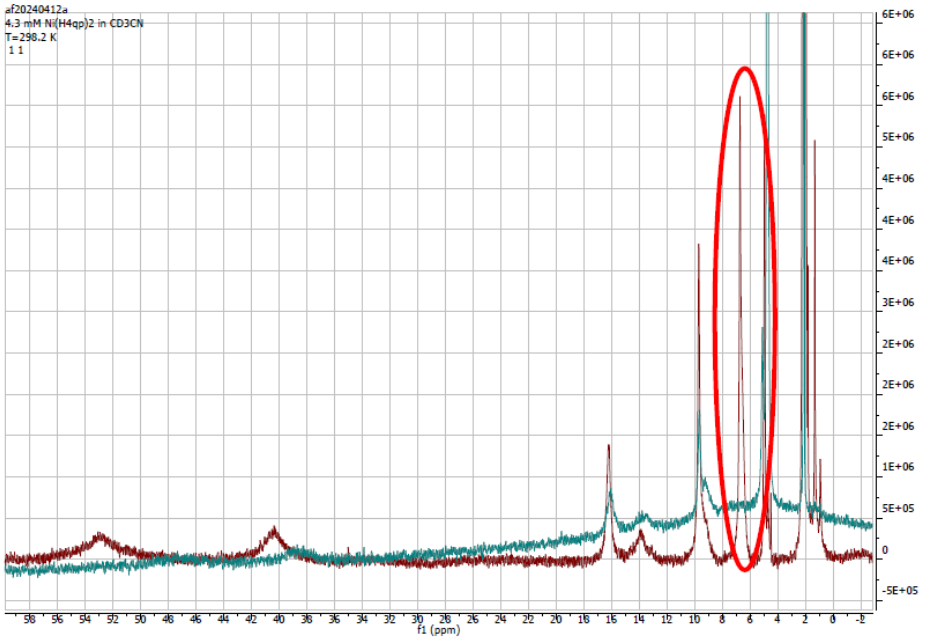

B

Figure S2. A) ^{1}H NMR data (400 mHz, 294 K) for a 4.3 mM sample of **2** in CD_3CN. B) Response of B) Comparison of data from panel A (brown) to spectrum obtained for 4.3 mM sample of **2** in 20% CD_3CN/80% D_2O (blue). The presence of D_2O causes the feature at 6.7 ppm to vanish.

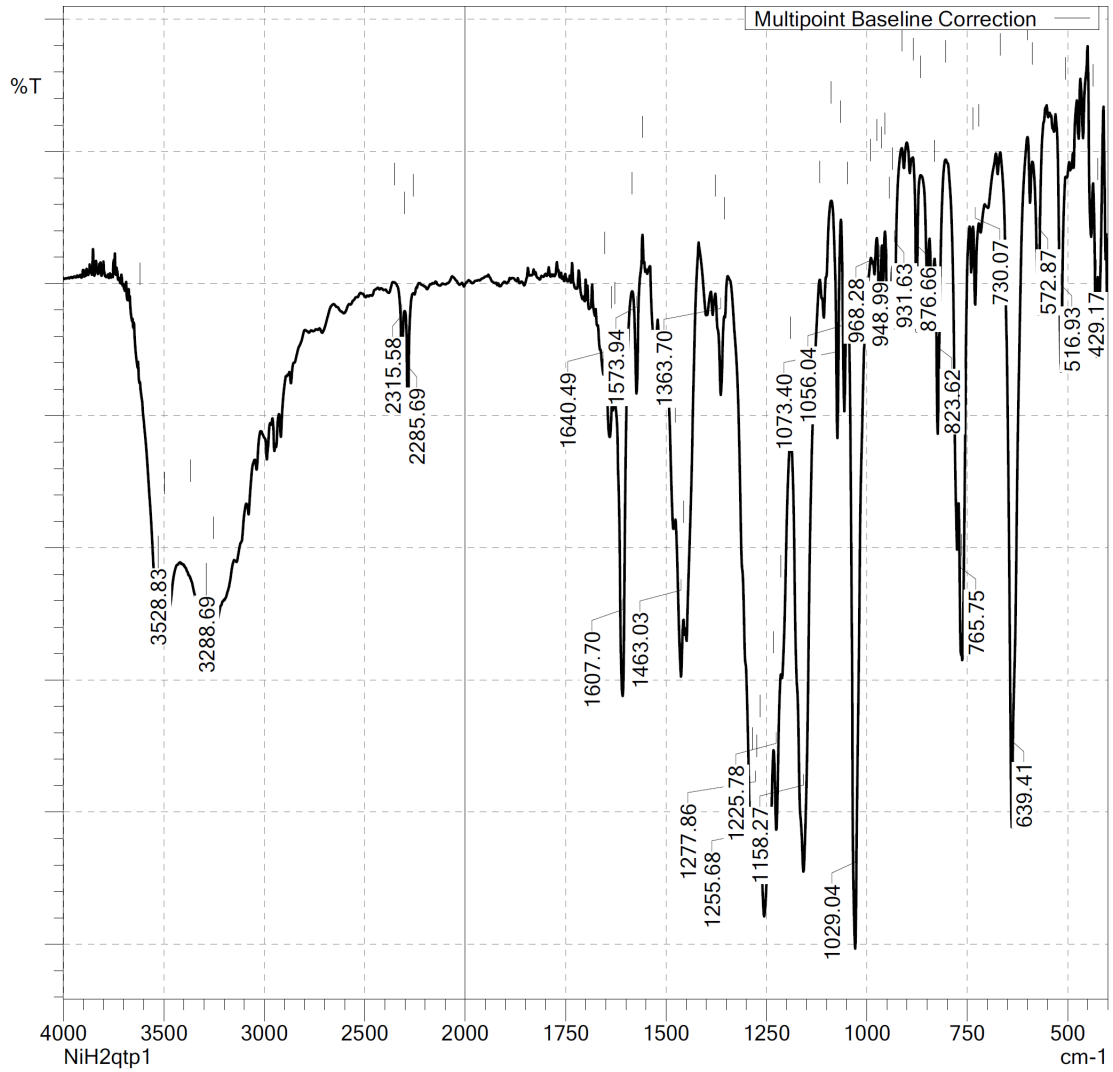

Figure S3. IR data (KBr) for [Ni(H_2qp1)(MeCN)](OTf)$_2$ (**1**).

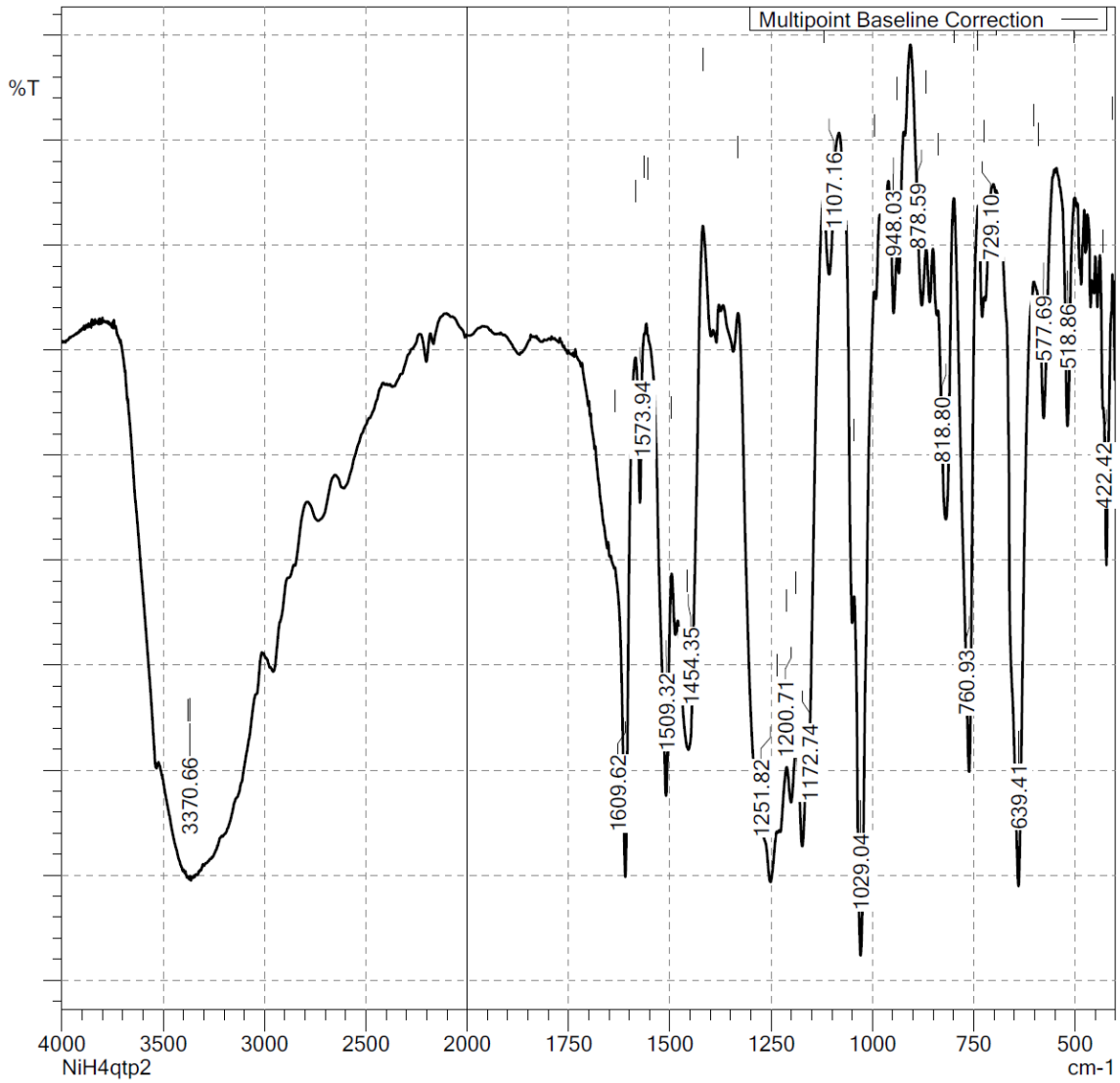

Figure S4. IR data (KBr) for $[Ni(H_4qp2)(MeCN)_2](OTf)_2$ (**2**).

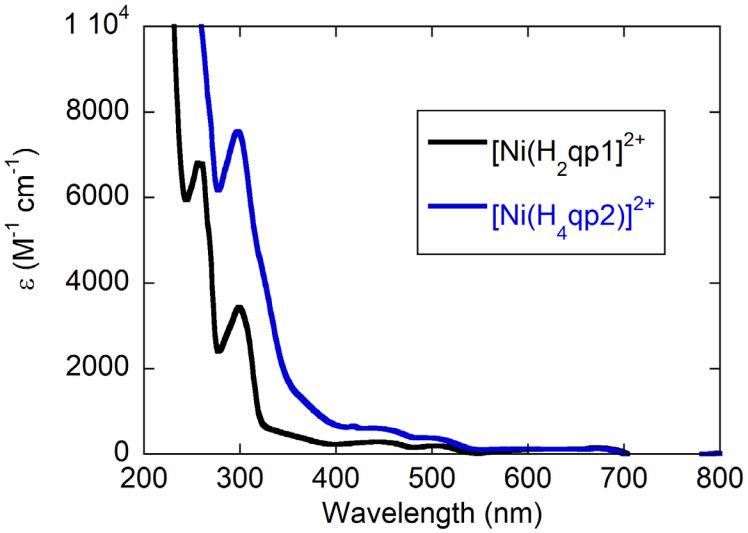

Figure S5. UV/vis data for **1** and **2**. The data for **1** were acquired for a 0.1 mM solution of the Ni(II) complex in MeOH whereas those for **2** were obtained using a 0.1 mM solution of the complex in MeCN. Both sets of data were obtained at 298 K using a 1.0 cm quartz cuvette. Observed peaks:

1 - 255 nm (6800 M^{-1} cm^{-1}), 299 nm (3430 M^{-1} cm^{-1}), 444 nm (285 M^{-1} cm^{-1}), 504 nm (195 M^{-1} cm^{-1}), 674 (150 M^{-1} cm^{-1})

2 - 298 nm (7550 M^{-1} cm^{-1}), 438 nm (610 M^{-1} cm^{-1}), 493 nm (380 M^{-1} cm^{-1}), and 668 (130 M^{-1} cm^{-1})

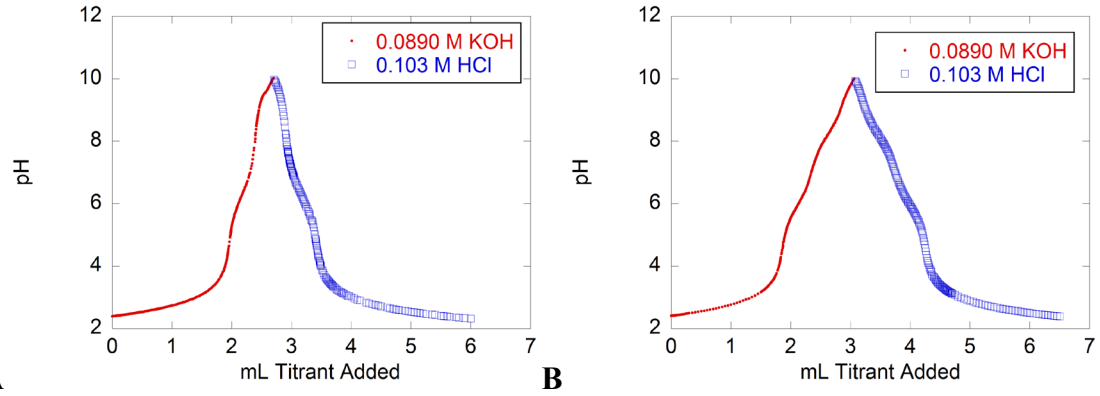

Figure S6. Potentiometric pH titration data for A) **1** and B) **2** in aqueous 100 mM KCl solutions. For the analysis of **1**, 0.10 mmol of H_2qtp1 and $Ni(OTf)_2$ were added to 48 mL of the KCl solution. 2.0 mL of 0.1018 M HCl was added to make the solution acidic, and the resultant mixture was subsequently titrated with 0.1008 M KOH (red data points). After 2.700 mL of KOH solution were added, the mixture was titrated with 0.1018 M HCl (blue data points). For the analysis of **2**, 0.10 mmol of H_4qtp2 and $Ni(OTf)_2$ were added to 50 mL of the KCl solution. 2.0 mL of 0.1018 M HCl was added to make the solution acidic, and the resultant mixture was subsequently titrated with 0.1008 M KOH (red data points). After 3.060 mL of KOH solution were added, the mixture was titrated with 0.1018 M HCl (blue data points). The data demonstrate that the titrations are reversible. Analyses of the data confirm a pK_a value of 6.33 (±0.05) for **1** and pK_a values of 5.99 (±0.05) and 8.24 (±0.05) for **2**.

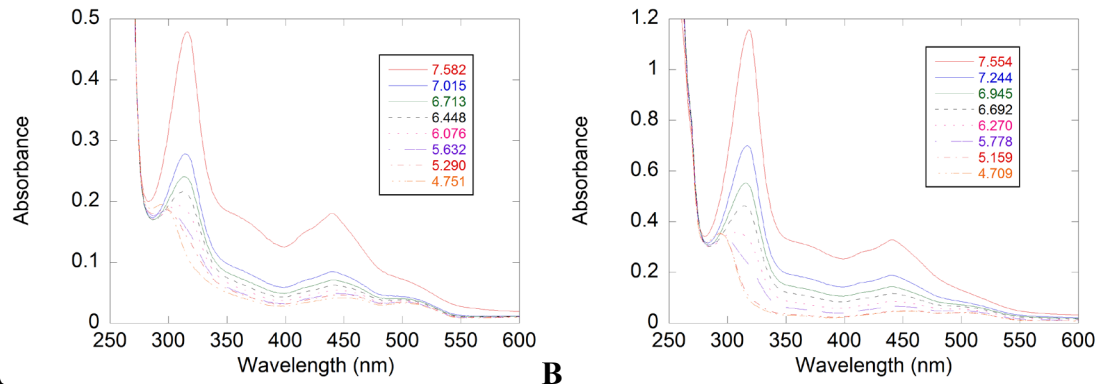

Figure S7. Spectrophotometric pH titration data for A) **1** and B) **2** in aqueous solutions. The data were acquired at 294 K with a 1.0 cm pathlength. The concentrations of Ni(II) and ligand in each sample were 0.10 mM. The pH was controlled through the addition of KOH and HCl. The peaks at 313 nm correspond to deprotonated quinols, whereas the peaks at 293-294 nm correspond to protonated quinols.

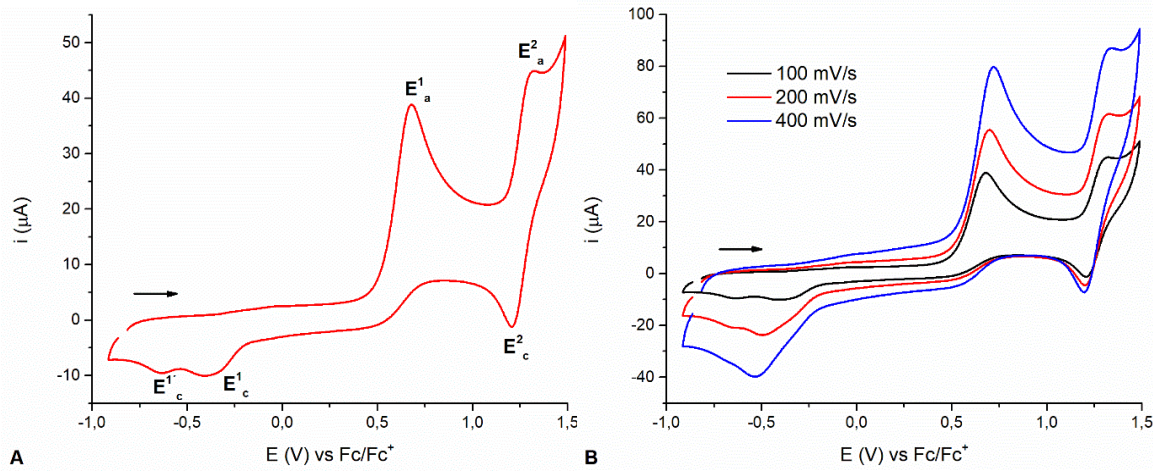

Figure S8. A) CV of 1.0 mM **1** in MeCN with 100 mM tetraethylammonium tetrafluoroborate ($TEABF_4$) at 100 mV/s. Features observed at E_a^1 = 680 mV, E_c^1 = -369 mV, and $E_c^{1'}$ = -629 mV correspond to the oxidation of the ligand to semiquinone. Features at E_a^2 = 1322 mV and E_c^2 = 1205 mV correspond to the oxidation to *para*-quinone. B) CV for the oxidation of 1.0 mM **1** to *para*-quinone in MeCN containing 100 mM $TEABF_4$ at different scan rates. The arrow shows the initial starting point and direction of the scans.

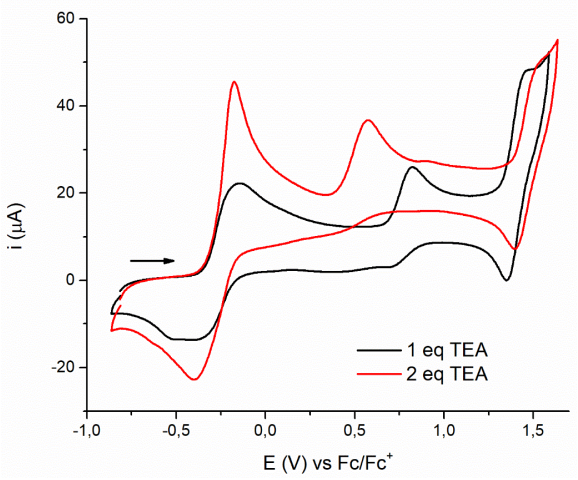

Figure S9. CV for 1.0 mM samples of **1** with 1.0 and 2.0 equiv. of triethylamine (TEA). Data were collected in MeCN containing 100 mM $TEABF_4$ with a 100 mV/s scan rate. The arrow shows the initial starting point and direction of the scans.

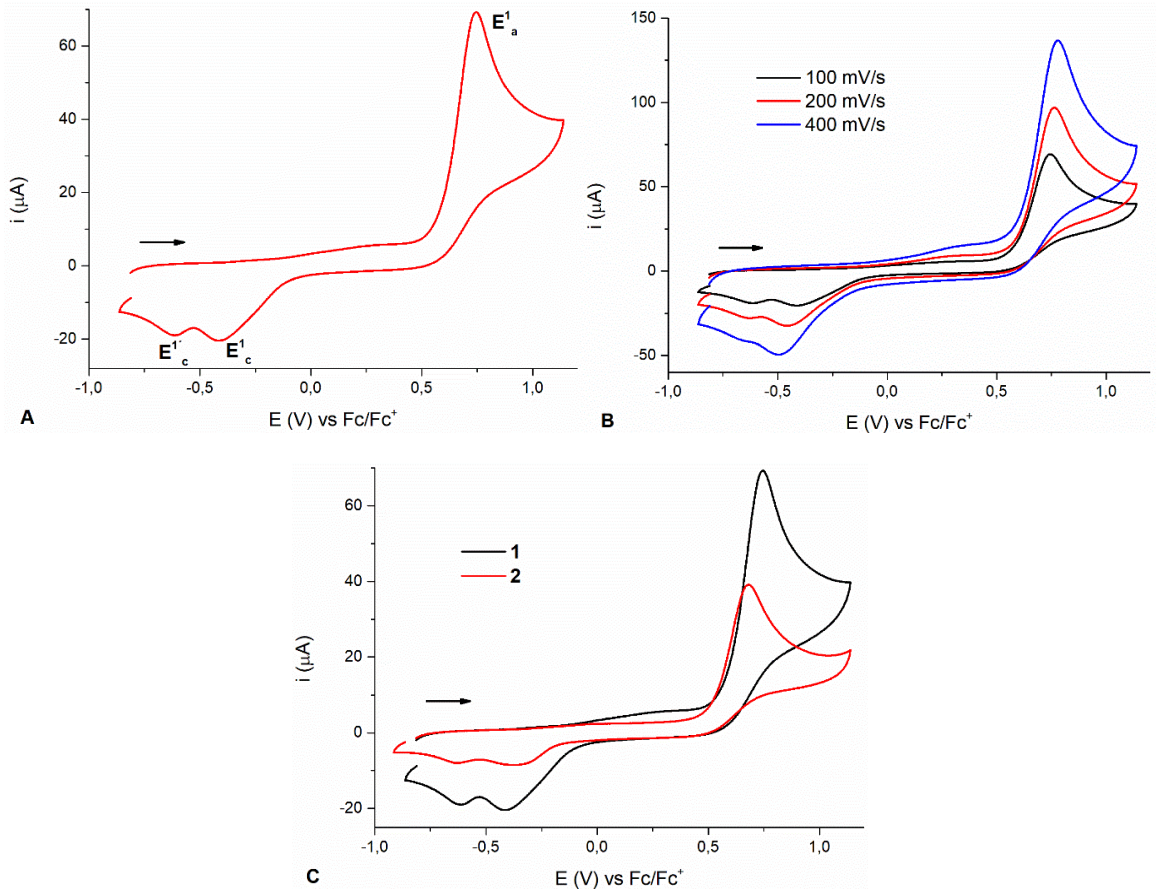

Figure S10. A) CV of 1.0 mM **2** in MeCN containing 100 mM $TEABF_4$ at 100 mV/s. The features at E_a^1 = 745 mV, E_c^1 = -411 mV, and $E_c^{1'}$ = -614 mV correspond to the oxidation of ligand oxidation to semiquinone and its subsequent reduction back to the quinol. B) CV for the oxidation of 1.0 mM **2** to semiquinone in MeCN containing 100 mM $TEABF_4$ at different scan rates. C) Comparison between the CVs of 1.0 mM **1** and 1.0 mM **2** in MeCN containing 100 mM $TEABF_4$ at 100 mV/s. . The arrows show the initial starting point and direction of the scans.

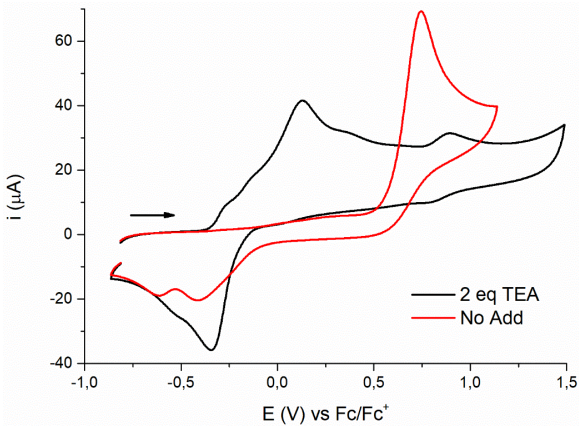

Figure S11. CV for 1.0 mM samples of **2** with 1.0 and 2.0 equiv. of TEA. Data were collected in MeCN containing 100 mM $TEABF_4$ with a 100 mV/s scan rate. The arrow shows the initial starting point and direction of the scans.

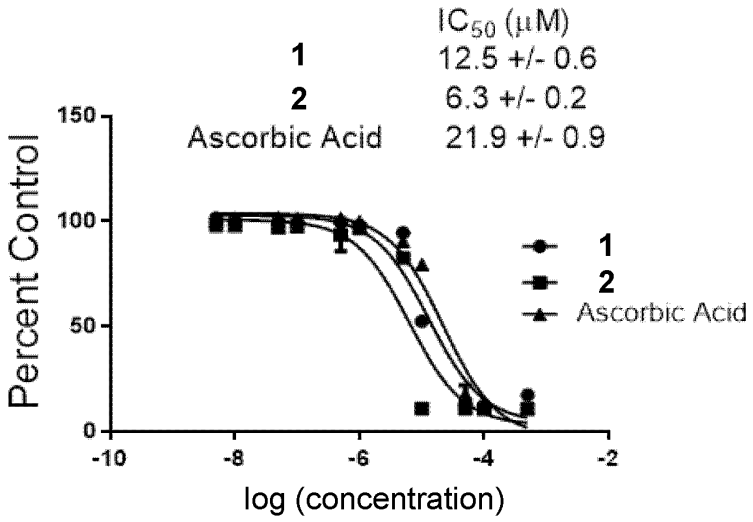

Figure S12. DPPH free radical scavenging assay of **1**, **2**, and ascorbic acid. The antioxidants were added to DPPH and incubated in the dark for 30 min at 298 K. Spectroscopic measurements were performed at 517 nm. The data were normalized to the absorbance in the presence of vehicle. All experiments were performed in triplicate and repeated twice.

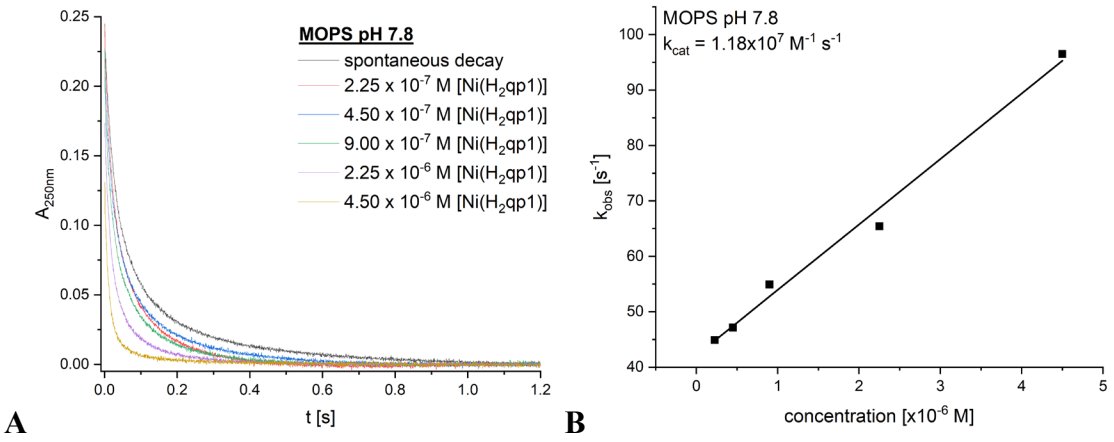

Figure S13. A) Kinetic traces of superoxide decomposition at 250 nm (60 mM MOPS buffer, pH 7.8, ionic strength of 150 mM) by **1.** B) Plot of k_{obs} vs. [**1**].

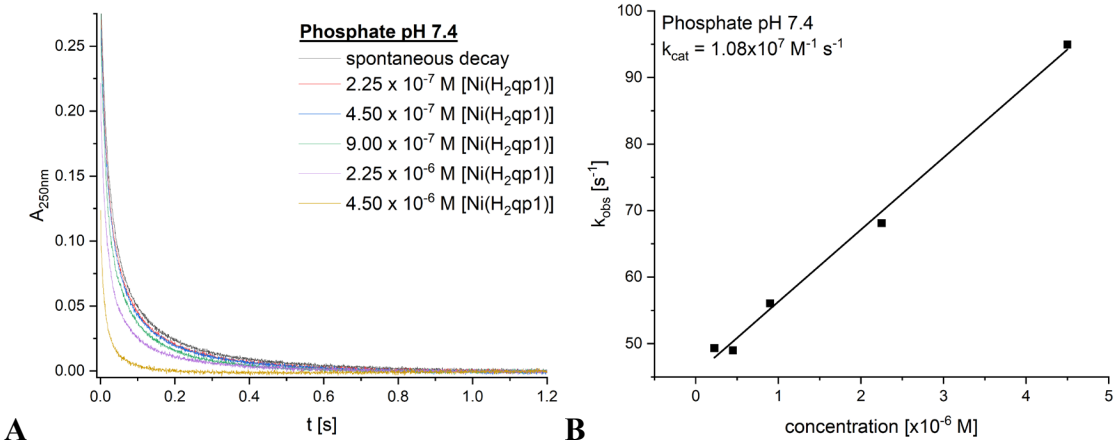

Figure S14. A) Kinetic traces of superoxide decomposition at 250 nm (50 mM phosphate buffer, pH 7.4, ionic strength of 150 mM) by **1.** B) Plot of k_{obs} vs. [**1**].

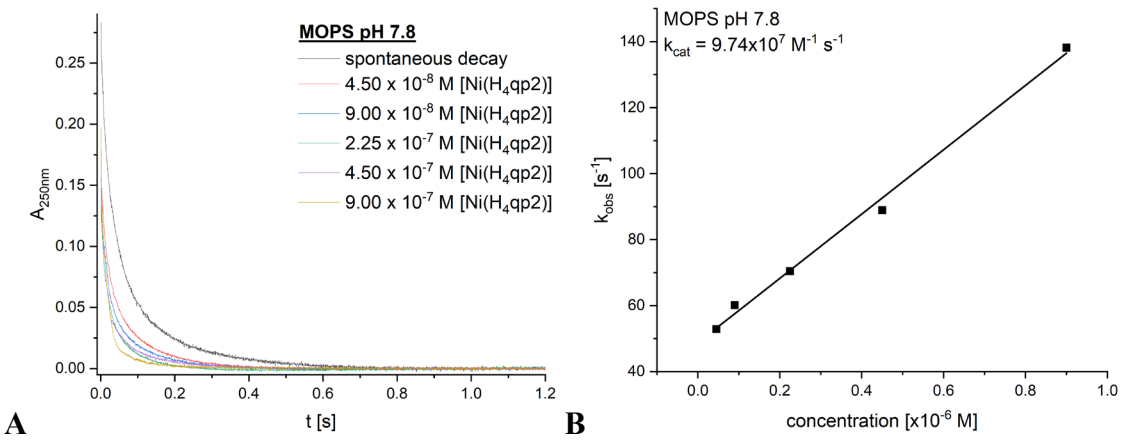

Figure S15. A) Kinetic traces of superoxide decomposition at 250 nm (60 mM MOPS buffer, pH 7.8 ionic strength of 150 mM) by **2.** B) Plot of k_{obs} vs. [**2**].

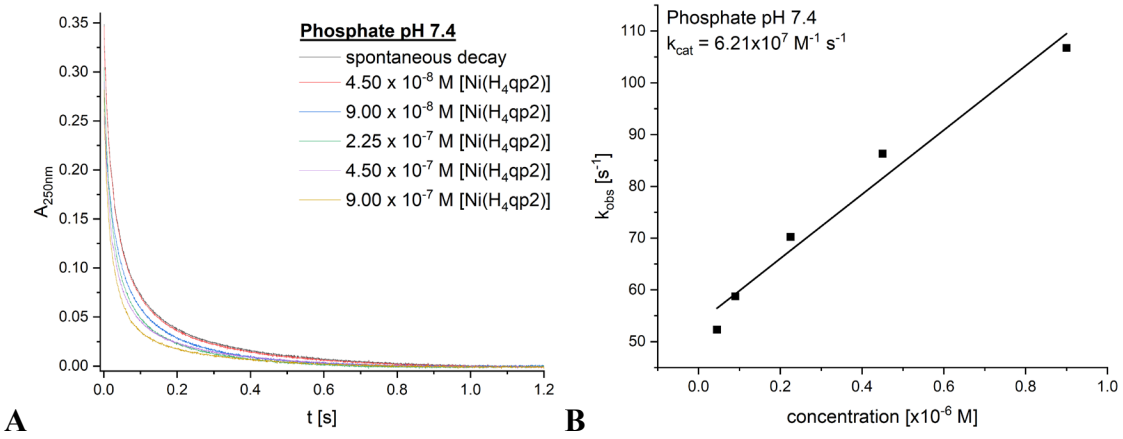

Figure S16. Kinetic traces of superoxide decomposition at 250 nm (50 mM phosphate buffer, pH 7.4, ionic strength of 150 mM) by **2.**

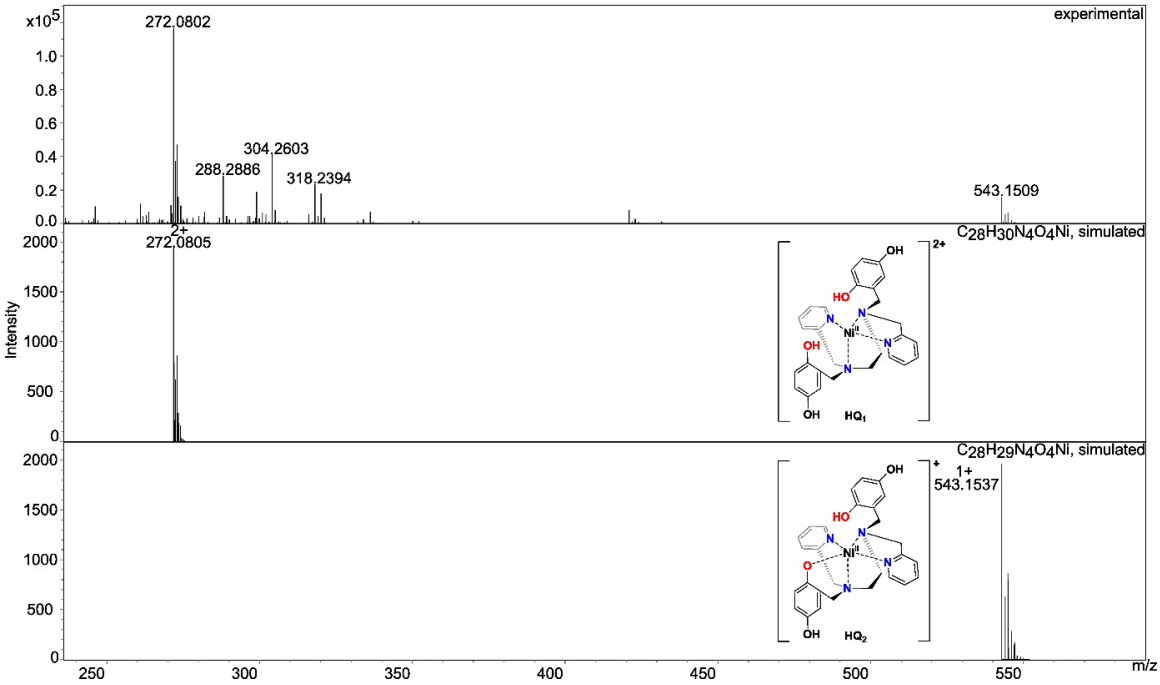

Figure S17. CSI-MS spectrometry of **2** prior to its reaction with KO_2. The graphics depict possible structures; we cannot preclude other modes of ligand coordination. Experimental conditions: a 1 mM solution of **2** in MeCN (1% DMF) was cooled to -40 °C, diluted in a pre-cooled syringe with pre-cooled MeCN to approximately 1×10^{-5} M, and quickly injected into the mass spectrometer. The predominant species are $[Ni^{II}(H_4qp2)]^{2+}$ (m/z = 272.0802) with a smaller amount of $[Ni^{II}(H_3qp2)]^{+}$ (m/z = 543.1537), where H_3qp2^- is the singly deprotonated form of the ligand.

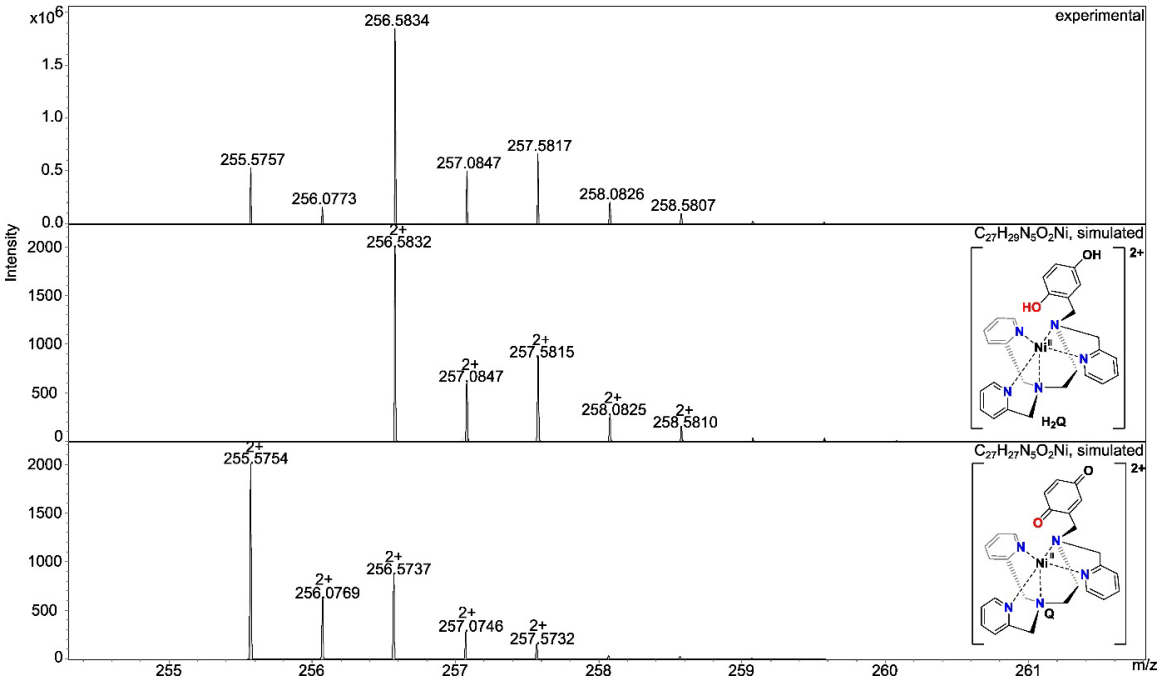

Figure S18. CSI-MS spectrometry of **1** prior to its reaction with KO_2. The graphics depict possible structures; we cannot preclude other modes of ligand coordination. Experimental conditions: a 1 mM solution of **1** in MeCN (1% DMF) was cooled to -40 °C, diluted in a pre-cooled syringe with pre-cooled MeCN to approximately 1×10^{-5} M, and quickly injected into the mass spectrometer. The predominant species are $[Ni^{II}(H_2qp1)]^{2+}$ (m/z = 256.5834) with a trace amount of $[Ni^{II}(qp1)]^{2+}$ (m/z = 255.5757), where *qp1* is the *para*-quinone form of the ligand.

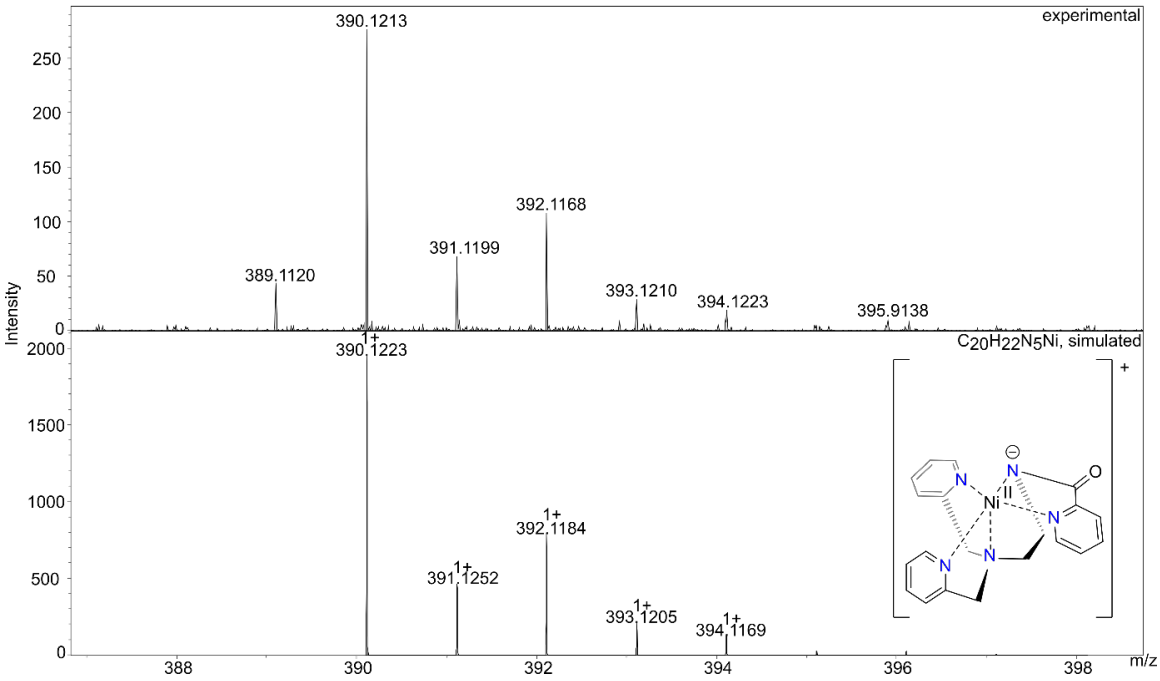

Figure S19. CSI-MS spectrometry of **1** after a 5 min reaction with KO_2. The graphics depict possible structures; we cannot preclude other modes of ligand coordination or sites of ligand oxidation. Experimental conditions: a 1 mM solution of **1** in MeCN (1% DMF) was cooled to -40 °C and then mixed with an excess of solid KO_2. Subsequently, the mixture was diluted in a pre-cooled syringe with pre-cooled MeCN to approximately 1×10^{-5} M and quickly injected into the mass spectrometer 5 min after the start of the reaction. The 390.1223 m/z peak is consistent with the loss of the quinol group and oxidation at one of the picolylic positions.

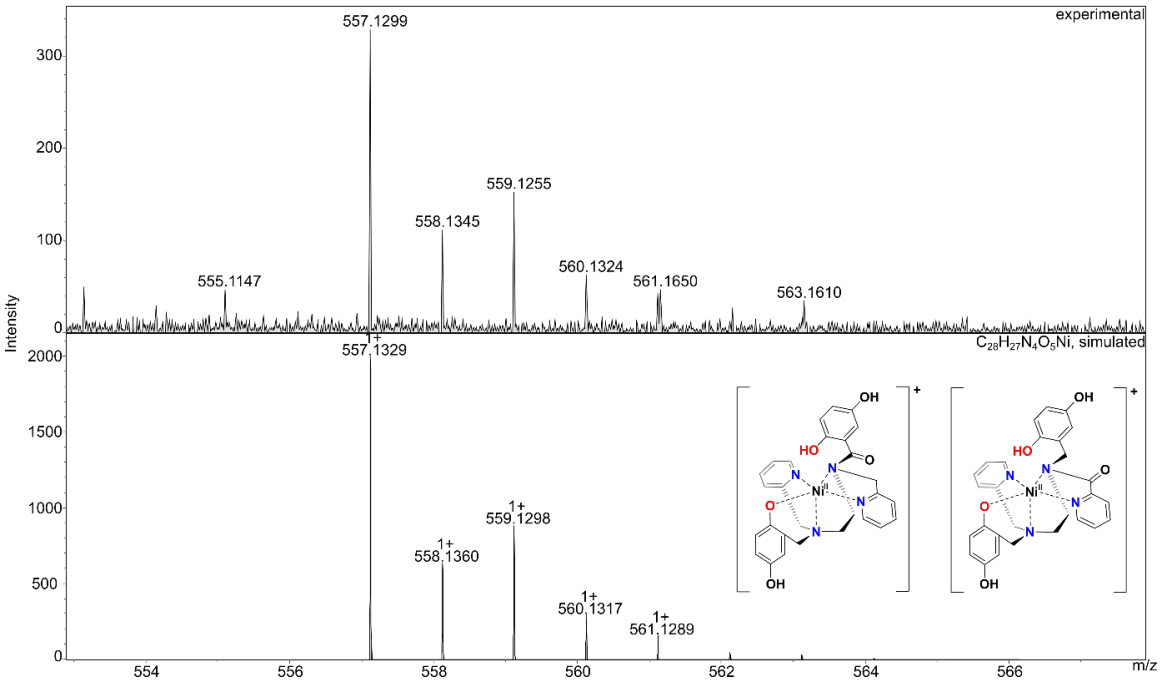

Figure S20. CSI-MS spectrometry of **2** after a 5 min reaction with KO_2. The graphics depict possible structures; we cannot preclude other modes of ligand coordination or sites of ligand oxidation. Experimental conditions: a 1 mM solution of **2** in MeCN (1% DMF) was cooled to -40 °C and then mixed with an excess of solid KO_2. Subsequently, the mixture was diluted in a pre-cooled syringe with pre-cooled MeCN to approximately 1×10^{-5} M and quickly injected into the mass spectrometer 5 min after the start of the reaction. The m/z peak at 557.1329 is consistent with oxidation at a benzylic or picoylic carbon.

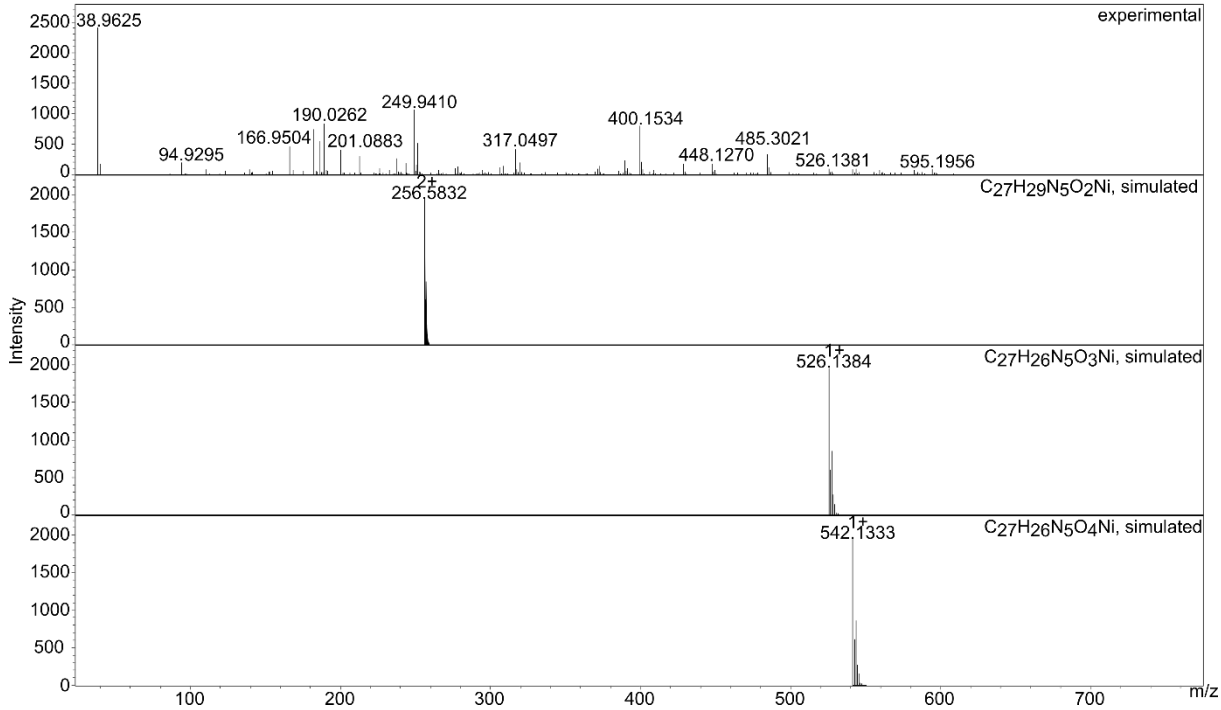

Figure S21. CSI-MS spectrometry of **1** after a sample from an extended reaction with KO_2 was warmed to room temperature (RT). Experimental conditions: a 1 mM solution of **1** in MeCN (1% DMF) was cooled to -40 °C and then mixed with an excess of solid KO_2. Subsequently, the mixture was diluted in a pre-cooled syringe with pre-cooled MeCN to approximately 1×10^{-5} M and allowed to warm to RT before injection into the mass spectrometer. The complex has undergone substantial degradation, and the products cannot be readily identified.

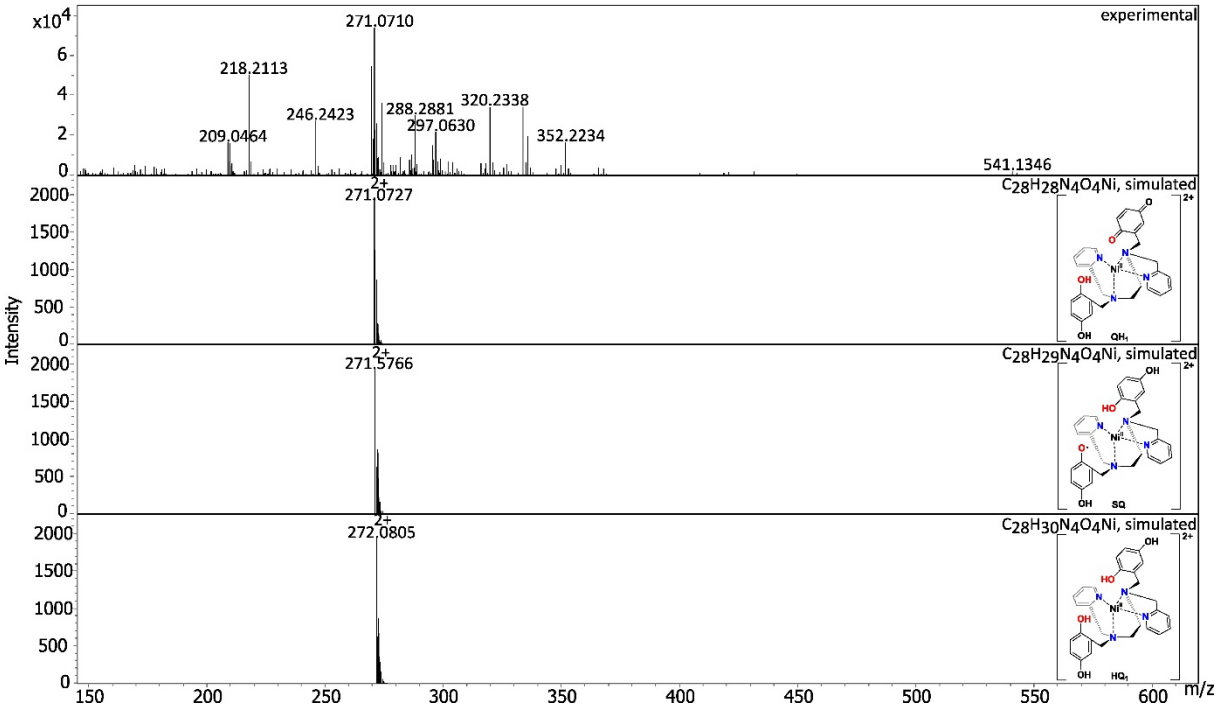

Figure S22. CSI-MS spectrometry of **2** after a sample from an extended reaction with KO_2 was warmed to RT. The graphics depict possible structures; we cannot preclude other modes of ligand coordination or sites of ligand oxidation.Experimental conditions: a 1 mM solution of **1** in MeCN (1% DMF) was cooled to -40 °C and then mixed with an excess of solid KO_2. Subsequently, the mixture was diluted in a pre-cooled syringe with pre-cooled MeCN to approximately 1×10^{-5} M and allowed to warm to RT before injection into the mass spectrometer.